arXiv:2505.02013v1 [cs.CV] 4 May 2025

MLLM-Enhanced Face Forgery Detection: A Vision-Language Fusion Solution

Siran Peng[1,2] **Zipei Wang**[1,2] **Li Gao**[3] **Xiangyu Zhu**[1,2]
Tianshuo Zhang[2,1] **Ajian Liu**[1,2] **Haoyuan Zhang**[2,1] **Zhen Lei**[1,2,4†]
[1]CASIA [2]UCAS [3]CMCC [4]CAIR, HKISI, CAS
{pengsiran2023,wangzipei2023,xiangyu.zhu,ajian.liu,zhanghaoyuan2023,zhen.lei}@ia.ac.cn
gaolids@chinamobile.com, tianshuo.zhang@nlpr.ia.ac.cn

Abstract

Reliable face forgery detection algorithms are crucial for countering the growing threat of deepfake-driven disinformation. Previous research has demonstrated the potential of Multimodal Large Language Models (MLLMs) in identifying manipulated faces. However, existing methods typically depend on either the Large Language Model (LLM) alone or an external detector to generate classification results, which often leads to sub-optimal integration of visual and textual modalities. In this paper, we propose VLF-FFD, a novel Vision-Language Fusion solution for MLLM-enhanced Face Forgery Detection. Our key contributions are twofold. First, we present EFF++, a frame-level, explainability-driven extension of the widely used FaceForensics++ (FF++) dataset. In EFF++, each manipulated video frame is paired with a textual annotation that describes both the forgery artifacts and the specific manipulation technique applied, enabling more effective and informative MLLM training. Second, we design a Vision-Language Fusion Network (VLF-Net) that promotes bidirectional interaction between visual and textual features, supported by a three-stage training pipeline to fully leverage its potential. VLF-FFD achieves state-of-the-art (SOTA) performance in both cross-dataset and intra-dataset evaluations, underscoring its exceptional effectiveness in face forgery detection.

1 Introduction

Recent breakthroughs in deepfake generation technology [1, 2, 3, 4, 5] have sparked widespread interest, primarily because of their capacity to create hyper-realistic synthetic faces that closely mimic genuine human features. Although these advancements hold promise for applications in entertainment and creative industries, they also introduce significant risks, including enabling fraud, amplifying misinformation, and creating deceptive fake news. Consequently, there is a pressing demand for accurate and reliable methods to detect facial forgeries and counteract their potential harm.

The rapid development of Multimodal Large Language Models (MLLMs) has greatly improved the alignment between visual and textual modalities [6, 7, 8, 9]. Recently, these models have been applied to face forgery detection, with an emphasis on generating explanatory insights. As shown in Figure 1, current MLLM-based methods typically adopt one of two strategies: (1) using the Large Language Model (LLM) to perform both classification and explanation [10, 11, 12, 13], or (2) incorporating an external detector for classification while utilizing the LLM for explanatory purposes [14]. However, both strategies rely on a single modality to deliver the classification results, which leads to sub-optimal integration of visual and textual information and, consequently, restricting overall performance.

To address this challenge, we propose VLF-FFD, a novel Vision-Language Fusion framework designed for MLLM-enhanced Face Forgery Detection. Our method consists of two main components. **First**, to facilitate more effective and informative MLLM training, we present EFF++, a frame-level,

Preprint. Under review.

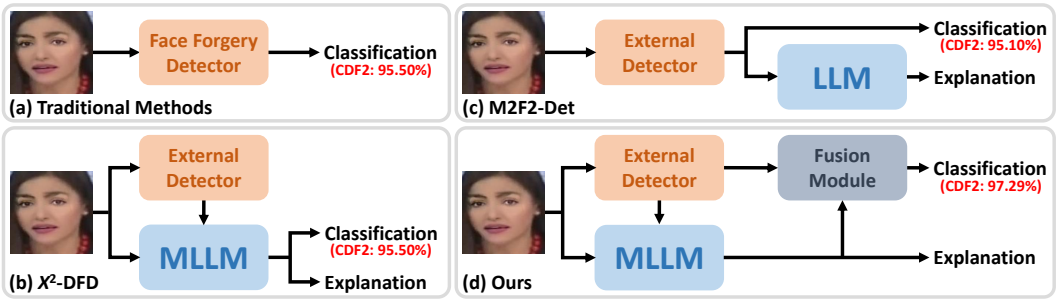

Figure 1: Comparative overview of face forgery detection frameworks evaluated on the Celeb-DeepFake-v2 (CDF2) benchmark [18]. **(a)** Traditional methods use face forgery detectors exclusively for classification, achieving a cross-dataset AUC of 95.50%. **(b)** $\mathcal{X}^2$-DFD [12], representing the first category of MLLM-based approaches, leverages an LLM (also MLLM) for both classification and explanation, also reaching 95.50% AUC. **(c)** M2F2-Det [14], belonging to the second category of MLLM-based methods, utilizes an external detector for classification and an LLM for explanation, achieving an AUC of 95.10%. **(d)** The proposed VLF-FFD enables bidirectional interaction between visual and textual modalities, delivering superior performance with a 97.29% AUC on CDF2.

explainability-driven extension of the FaceForensics++ (FF++) dataset [15], leveraging a commercial LLM [16]. Specifically, we introduce the Contrastive Forgery Artifacts Discovery (CFAD) method, which precisely identifies facial forgery clues by providing the commercial LLM with paired real and fake face images. Additionally, we expand the dataset by incorporating the Manipulation Technique Summarization (MTS) approach, which distills the manipulation strategies outlined in the original FF++ paper. As a result, for each manipulated video frame, EFF++ provides a paired textual annotation that describes both the forgery artifacts and the specific manipulation technique used. **Second**, we design a Vision-Language Fusion Network (VLF-Net) that promotes bidirectional interaction between visual and textual features. Our network architecture comprises an external detector [17], an MLLM [8], and an innovative Vision-Language Fusion Module (VLFM). The external detector directly extracts visual features from the input image, while the MLLM processes both the input image and the visual feature map produced by the external detector to generate text embeddings and provide explanatory content. Finally, the VLFM integrates these visual and textual representations to generate the final classification result. To maximize the performance of VLF-Net, we employ a three-stage training pipeline: (1) training the external detector independently to ensure robust visual feature extraction, (2) freezing the external detector and training the MLLM to enhance textual representations, and (3) freezing both the external detector and the MLLM while training the VLFM to optimize the fusion process. In conclusion, the **contributions** of this paper are as follows:

- We present EFF++, a frame-level, explainability-driven extension of the FF++ dataset. In EFF++, each manipulated video frame is paired with a textual annotation describing both the forgery artifacts and the manipulation technique, facilitating more informative training of the MLLM.
- We introduce VLF-Net, a novel architecture that integrates an external detector, an MLLM, and a fusion module to promote bidirectional interaction between visual and textual features. Additionally, we employ a three-stage training pipeline to maximize the potential of this network.
- The proposed VLF-FFD, consisting of the EFF++ dataset and the VLF-Net architecture, demonstrates state-of-the-art (SOTA) performance in both cross-dataset and intra-dataset evaluations, highlighting its exceptional effectiveness in the field of face forgery detection. Furthermore, comprehensive ablation studies validate the robustness and correctness of our design choices.

2 Related Works

2.1 Traditional Face Forgery Detection

Face forgery detection is traditionally framed as a binary classification problem, where a model is trained to assess whether an image or video is "real" or "fake". As outlined in [19], these detection

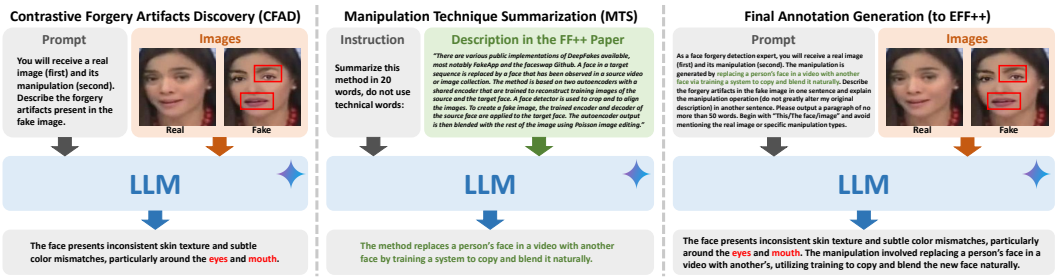

Figure 2: Annotation for a fake video frame from the EFF++ dataset. CFAD is employed to identify and explain facial forgeries, while MTS is used to extract and summarize the specific manipulation strategy applied. The combination of these methods results in an informative textual annotation.

methods can be broadly divided into four categories: spatial-domain, time-domain, frequency-domain, and data-driven approaches. Spatial-domain techniques identify facial forgeries by analyzing inherent spatial features within an image, such as color inconsistencies [20], saturation variations [21], and the presence of artifacts [22, 23, 24, 25, 26]. Time-domain methods, on the other hand, detect manipulations across temporal sequences by examining inter-frame inconsistencies, leveraging the entire video for analysis [27, 28, 29, 30, 31, 32, 33]. Frequency-domain techniques convert spatial or temporal data into the frequency domain using algorithms such as Fast Fourier Transform (FFT) [34], Discrete Cosine Transform (DCT) [35, 36], and Discrete Wavelet Transform (DWT) [37, 38, 39, 40]. These approaches excel at revealing subtle forgery traces that may not be visible in the spatial or temporal domains. Lastly, data-driven methods refine network architectures and optimize training strategies, fully harnessing the potential of available data to improve detection performance [41, 42, 43, 44, 45, 46, 47]. However, the approaches mentioned above only deliver classification results without offering any explanations for their decisions, which limits their interpretability.

2.2 MLLM-based Face Forgery Detection

Vision and language represent two of the most powerful modalities in Artificial Intelligence (AI). Recent advancements in MLLMs, particularly the LLaVA series [7, 8, 9], have significantly enhanced the alignment and integration of visual and textual data. These models are now being actively leveraged for face forgery detection, with a key emphasis on providing explanatory insights [10, 11, 48, 49, 50]. Current MLLM-based detection methods can be roughly classified into two categories, depending on how they produce classification results. The first category utilizes the LLM to handle both classification and explanation tasks simultaneously. Notable examples include $\mathcal{X}^2$-DFD [12] and KFD [13]. In $\mathcal{X}^2$-DFD, the output score from an external detector is integrated into the prompt to fine-tune the LLM, enabling it to generate both classification results and explanations. Similarly, KFD transforms the outputs of the external detector into prompt embeddings, which fine-tune the LLM to produce the final classification and explanation. The second category incorporates an external detector for classification, while the LLM is employed to generate explanations. A prominent example in this category is M2F2-Det [14], which uses a CLIP-based [51] detector to produce classification results and prompt embeddings. These embeddings then guide the LLM in generating explanations. However, methods in both categories rely on a single modality for final classification, leading to sub-optimal integration of visual and textual information, which ultimately limits the overall performance.

3 Methodology

3.1 EFF++

EFF++ is a frame-level, explainability-driven extension of the FF++ dataset [15], developed using Gemini 2.0[1], a commercial LLM with advanced multimodal alignment capabilities [52]. In EFF++, each manipulated video frame is accompanied by a textual annotation that describes both the forgery artifacts and the specific manipulation technique applied. As illustrated in Figure 2, these annotations are generated through two novel methods: Contrastive Forgery Artifacts Discovery (CFAD), which

[1] `https://gemini.google.com`

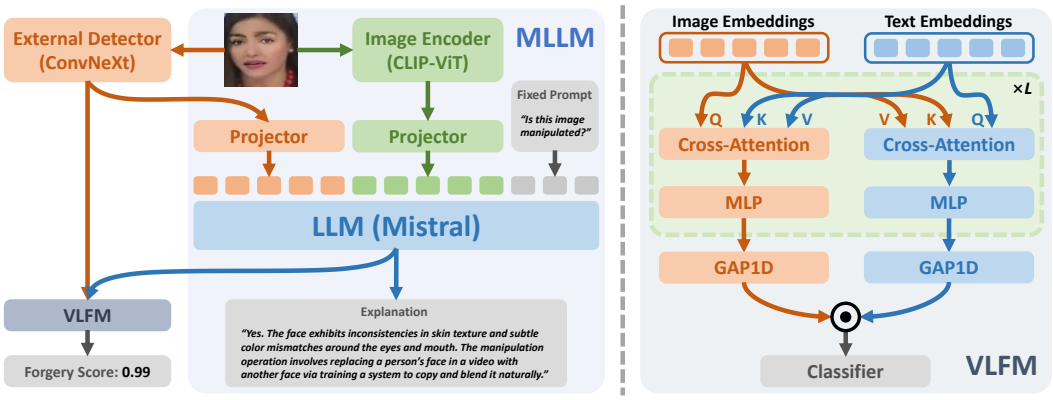

Figure 3: Overview of the VLF-Net architecture. The network consists of three main components: (1) an external detector, (2) an MLLM that includes an image encoder, two projectors, and an LLM, and (3) the innovative Vision-Language Fusion Module (VLFM). VLF-Net facilitates bidirectional interaction between visual and textual information. GAP1D refers to Global Average Pooling 1D.

identifies and explains facial forgeries, and Manipulation Technique Summarization (MTS), which concisely summarizes the manipulation strategies employed. The following section introduces CFAD and MTS and explains how they are integrated to produce the final textual annotations in EFF++.

CFAD. Unlike previous methods that provide the LLM with only the manipulated image [53, 12], we supply both the original and manipulated images to the LLM. Specifically, for each identity, we extract frames and crop faces from both the original video and its four manipulated counterparts, following the procedure detailed in Appendix A.1. This yields a set of image pairs denoted as $\mathcal{S} = \{(I_R^i, I_F^{i,j}) \mid i = 1, ..., N;\ j = 1, ..., 4\}$, where I_R and I_F represent the real and fake images, respectively, and N is the total number of frames. Subsequently, each image pair $(I_R^i, I_F^{i,j})$ is fed into the LLM, along with a prompt that clarifies the relationship between the two images and requests an explanation of any facial forgery clues present in the manipulated image. By enabling a direct visual comparison, CFAD empowers the LLM to more precisely identify and localize forgery artifacts.

MTS. To enrich our dataset with more authoritative information beyond basic common-sense reasoning (e.g., [53, 12]), we incorporate brief explanations of the four FF++ manipulation techniques. Specifically, we extract the official descriptions of Deepfakes (DF), Face2Face (F2F) [54], FaceSwap (FS), and NeuralTextures (NT) [55] from the FF++ paper. These are then provided to the LLM, which is instructed to generate clear, non-technical summaries. This process yields four one-sentence explanations, each capturing the essence of a specific manipulation strategy in language accessible to a broad audience. Both the original descriptions and the summaries are included in Appendix A.2.

Final Annotation Generation. In EFF++, each manipulated video frame is annotated using a combination of the CFAD and MTS methods. Specifically, we embed the MTS-generated summary (shown as green text in Figure 2) within the CFAD's prompting framework. To further enhance the annotation process, we introduce supplemental instructions that (1) encourage subtle rephrasing of the summary description and (2) enforce a standardized output format. This approach ensures that each textual annotation captures both the forgery artifacts and the manipulation technique in a flexible yet consistent manner. For each real video frame, we employ a straightforward prompt that instructs the LLM to articulate the frame's natural, unmodified characteristics. Additional examples from the EFF++ dataset, as well as the prompt used for annotating real frames, are available in Appendix A.3. Lastly, each annotation is prefixed with "Yes" (for manipulated video frames) or "No" (for real video frames), followed by the question, "Is this image manipulated?", thereby forming the EFF++ dataset.

3.2 VLF-Net

Overall Architecture. The VLF-Net, as illustrated in Figure 3, is composed of three main components: an external detection, an MLLM, and the proposed Vision-Language Fusion Module (VLFM). For the external detector, we choose the widely used ConvNeXt architecture [17], which excels at capturing fine-grained visual features. The MLLM, built upon the LLaVA framework [8], includes

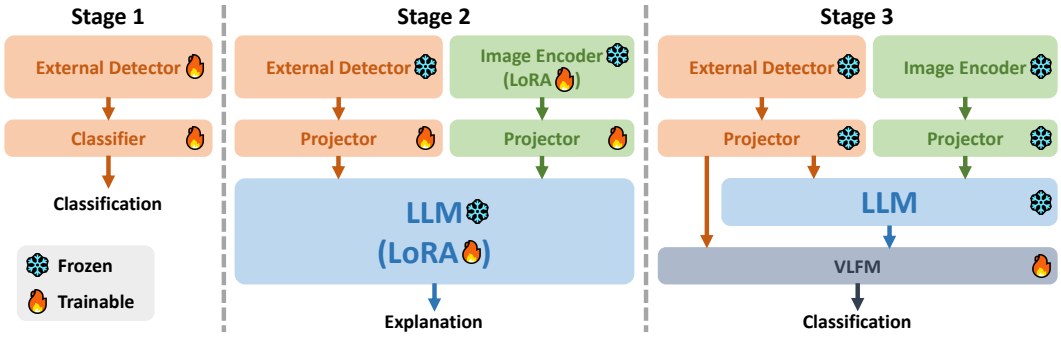

Figure 4: Overview of the three-stage training pipeline for VLF-Net. In Stage 1, the external detector is trained independently. In Stage 2, the external detector is frozen while the MLLM is fine-tuned. In Stage 3, both the external detector and the MLLM are frozen, and the VLFM is trained.

an image encoder (CLIP-ViT [51]), two projectors, and an LLM (Mistral [56]). The VLFM, an innovative fusion structure, will be explained later. Given an input image, VLF-Net simultaneously processes it through the external detector and the image encoder, producing a visual feature map and ViT image embeddings, denoted as E_V. The visual feature map is then flattened across its spatial dimensions to generate ConvNeXt image embeddings, E_C. Subsequently, two distinct projectors map E_V and E_C into a text embedding space. These projected embeddings are concatenated with fixed prompt embeddings and passed to the LLM, which outputs text embeddings, E_L, as well as explanatory content. Finally, the VLFM integrates E_C and E_L to produce the classification result.

VLFM. As depicted in Figure 3, the VLFM receives image embeddings $E_C \in \mathbb{R}^{n_c \times d}$ and text embeddings $E_L \in \mathbb{R}^{n_l \times d}$ as inputs, where n_c and n_l denote the number of image and text tokens, respectively, and d is the embedding dimension. To facilitate effective multimodal classification, VLFM employs a series of cross-modal fusion layers, each consisting of two complementary cross-attention mechanisms: an image-to-text block and a text-to-image block, along with corresponding Multi-Layer Perceptrons (MLPs). The image-to-text cross-attention block, $\mathrm{CA}_{\mathrm{img}\to\mathrm{text}}$, treats image embeddings E_C as Queries (Q) and text embeddings E_L as Keys (K) and Values (V), computed as:

$$\mathrm{CA}_{\mathrm{img}\to\mathrm{text}}(E_C, E_L) = \mathrm{softmax}\left(\frac{E_C W^Q (E_L W^K)^\top}{\sqrt{d}}\right)(E_L W^V), \tag{1}$$

where $W^Q, W^K, W^V \in \mathbb{R}^{d\times d}$ are learnable projection metrics. Conversely, the text-to-image cross-attention block, $\mathrm{CA}_{\mathrm{text}\to\mathrm{img}}$, uses text embeddings E_L as Q and image embeddings E_C as K and V:

$$\mathrm{CA}_{\mathrm{text}\to\mathrm{img}}(E_L, E_C) = \mathrm{softmax}\left(\frac{E_L W^Q (E_C W^K)^\top}{\sqrt{d}}\right)(E_C W^V). \tag{2}$$

Each cross-attention output is subsequently refined by an MLP. The VLFM comprises L cross-modal fusion layers, progressively enhancing the integration of visual and textual features. Following the final fusion layer, the output embeddings are aggregated through Global Average Pooling 1D (GAP1D) and combined using a dot-product operation to produce a joint representation Z:

$$Z = \mathrm{GAP1D}(E_C^{(L)}) \odot \mathrm{GAP1D}(E_L^{(L)}), \tag{3}$$

where $E_C^{(L)}$ and $E_L^{(L)}$ represent the image and text embeddings after L fusion layers, and $\odot$ denotes the dot-product. The joint representation Z is then fed into a classifier to generate the final prediction.

Training Pipeline. We develop a three-stage training pipeline to maximize the performance of VLF-Net, as shown in Figure 4. In Stage 1, we train the external detector independently using standard Cross-Entropy (CE) Loss to extract visual features. In Stage 2, the external detector is frozen, and the MLLM is trained with Supervised Fine-Tuning (SFT) Loss to enhance textual representations. During this stage, both the image encoder and LLM are fine-tuned using Low-Rank Adaptation (LoRA) [57], while the projectors undergo full training. Finally, in Stage 3, we freeze both the external detector and the MLLM, and train the VLFM with CE Loss to integrate visual and textual information.

Table 1: Cross-dataset performance comparison of SOTA face forgery detection methods on the CDF2, DFDC, DFDCP, and FFIW benchmarks. Methods with $*$ are reproduced using their official codes, while results for others are taken from the original papers. The highest performance for each dataset is shown in **bold**, and the second-best is underlined. Methods above the central dividing line are traditional approaches, while those below are MLLM-based. Notably, VLF-FFD consistently outperforms other methods across all datasets, demonstrating its superior generalization capability.

Method	Venue	Explainable	Test Set AUC (%)			
			CDF2	DFDC	DFDCP	FFIW
F^3-Net* [35]	ECCV 2020	✗	77.92	67.35	73.54	70.11
LTW* [58]	AAAI 2021	✗	77.14	69.00	74.58	76.63
PCL+I2G [41]	ICCV 2021	✗	90.03	67.52	74.37	-
DCL [59]	AAAI 2022	✗	82.30	-	76.71	71.14
SBI [24]	CVPR 2022	✗	93.18	72.42	86.15	84.83
F^2Trans [39]	TIFS 2023	✗	89.87	-	76.15	-
AUNet [60]	CVPR 2023	✗	92.77	73.82	86.16	81.45
SeeABLE [61]	ICCV 2023	✗	87.30	75.90	86.30	-
LAA-Net [62]	CVPR 2024	✗	95.40	-	86.94	-
RAE [63]	ECCV 2024	✗	<u>95.50</u>	80.20	89.50	-
FreqBlender [64]	NeurIPS 2024	✗	94.59	74.59	87.56	86.14
UDD [65]	AAAI 2025	✗	93.10	81.20	88.10	-
LESB [66]	WACVW 2025	✗	93.13	71.98	-	83.01
$\mathcal{X}^2$-DFD [12]	arXiv 2024	✓	<u>95.50</u>	<u>85.30</u>	91.20	-
KFD [13]	arXiv 2025	✓	94.71	79.12	<u>91.81</u>	-
M2F2-Det [14]	arXiv 2025	✓	95.10	-	87.80	<u>88.70</u>
VLF-FFD (Ours)	-	✓	**97.29**	**85.41**	**92.04**	**89.15**

4 Experiments

4.1 Setup

Datasets. We conduct model training and intra-dataset evaluation on the widely recognized FaceForensics++ (FF++) benchmark [15], which comprises 1,000 real face videos and 4,000 fake videos generated by four forgery techniques: DeepFakes (DF), Face2Face (F2F) [54], FaceSwap (FS), and NeuralTextures (NT) [55]. Our three-stage training pipeline utilizes the FF++ dataset as follows: for cross-dataset assessment, we adhere to the SBI framework [24] and employ only real FF++ samples during Stages 1 and 3; for intra-dataset assessment, both real and fake samples are used in these stages. In both cases, Stage 2 leverages the proposed EFF++ dataset, an explainability-driven extension of FF++, to enhance model interpretability. Cross-dataset performance is evaluated on four challenging datasets: Celeb-DeepFake-v2 (CDF2) [18], which applies advanced deepfake methods to YouTube celebrity videos; the DeepFake Detection Challenge (DFDC) [67] and its Preview version (DFDCP) [68], both of which introduce diverse perturbations such as compression, downsampling, and noise; and FFIW-10K (FFIW) [69], which increases complexity by including multi-person scenarios.

Baselines. We evaluate our approach against eighteen representative baselines for face forgery detection, including fifteen traditional methods and three MLLM-based techniques (introduced in Section 2.2). The traditional baselines encompass a diverse range of strategies: Face X-ray [70] introduces a grayscale representation to reveal blend boundaries, while F^3-Net [35] utilizes frequency-aware clues to identify manipulations. LTW [58] emphasizes domain-general robustness, and PCL+I2G [41] targets source-feature inconsistencies. DCL [59] exploits multi-granular contrastive learning for enhanced representation, whereas SBI [24] augments training with synthetically generated fake faces. SOLA [71] is designed to reduce local feature anomalies for improved generalization, and F^2Trans [39] fuses spatial and frequency domain traces to capture forgery artifacts. AUNet [60] investigates facial Action Unit (AU) regions for more nuanced analysis, and SeeABLE [61] reframes forgery detection as an Out-Of-Distribution (OOD) challenge. LAA-Net [62] introduces heatmap-

Table 2: Intra-dataset performance comparison of SOTA face forgery detection methods. For clarity, only the top-performing results are highlighted. VLF-FFD achieves the best overall performance.

Method	Venue	Test Set AUC (%)				
		DF	F2F	FS	NT	FF++
Face X-ray* [70]	CVPR 2020	99.12	99.31	99.09	99.27	99.20
PCL+I2G [41]	ICCV 2021	**100.00**	99.57	**100.00**	99.58	99.79
SOLA [71]	CVPR 2022	**100.00**	99.67	**100.00**	99.82	99.87
AUNet [60]	CVPR 2023	**100.00**	99.86	99.98	99.71	99.89
RAE [63]	ECCV 2024	99.60	99.10	99.20	97.60	98.90
VLF-FFD (Ours)	-	**100.00**	**99.89**	**100.00**	**99.73**	**99.91**

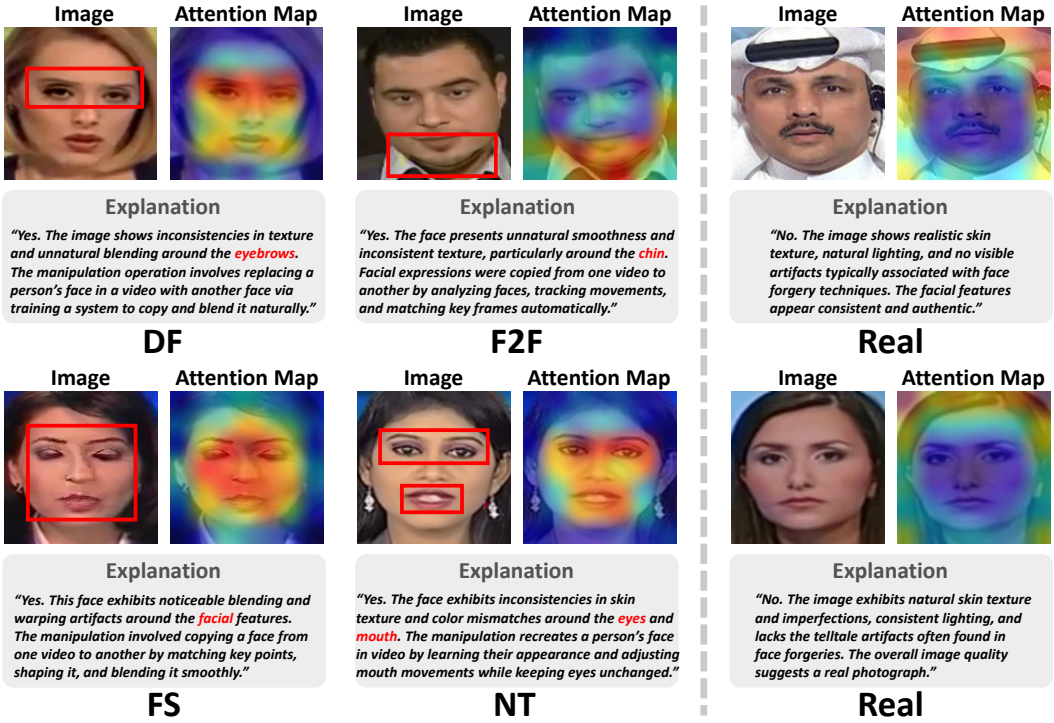

Figure 5: Attention maps generated by VLFM alongside their corresponding explanatory outputs for examples from the FF++ dataset. The attention maps highlight facial regions containing forgery artifacts, closely matching the areas mentioned in the explanatory contents. Notably, this visualization demonstrates the strong alignment between visual and textual modalities achieved by VLF-FFD.

guided self-consistency attention, while RAE [63] focuses on recovering authentic facial appearances from perturbations. FreqBlender [64] generates pseudo-fake faces by blending frequency knowledge, UDD [65] mitigates position and content biases through a dual-branch architecture, and LESB [66] employs a Local Feature Discovery (LFD) mechanism to create self-blended samples. Collectively, these baselines provide a comprehensive comparison framework for assessing the proposed method.

Evaluation Metric. Detection performance is evaluated using the Area Under the Receiver Operating Characteristic Curve (AUC), which is the standard metric for assessing face forgery detection. We report results at the video level by averaging predictions across all frames within each video.

Implementation Details. This work leverages the preprocessing techniques, data augmentation strategies, and testing pipeline developed by SBI [24]. For the external detector, we employ ConvNeXt-B-224 [17] as the backbone, pre-trained on the ImageNet-1K dataset [72]. The MLLM is based on LLaVA-v1.6-Mistral-7B [8], which utilizes CLIP-ViT-L/14-336 [51] as the image encoder and Mistral-7B [56] as the LLM. Additionally, the number of cross-modal fusion layers L is set to 2.

Table 3: Ablation study results for the EFF++, showcasing its effectiveness in boosting detection performance compared to alternative datasets.

Dataset	Test Set AUC (%)				Avg.
	CDF2	DFDC	DFDCP	FFIW	
DDVQA [53]	96.90	84.86	91.65	88.87	90.57
w/o CFAD & MTS	97.12	85.11	91.70	88.99	90.73
w/o CFAD	97.09	85.03	91.76	89.14	90.76
w/o MTS	97.25	85.32	91.85	**89.21**	90.91
EFF++ (Ours)	**97.29**	**85.41**	**92.04**	89.15	**90.97**

Table 4: Ablation study results for MLLM, highlighting the performance improvements obtained by incorporating MLLM into our framework.

Method	Test Set AUC (%)				Avg.
	CDF2	DFDC	DFDCP	FFIW	
Pre-trained LLaVA	51.32	56.54	56.03	55.70	54.90
Fine-tuned LLaVA	76.99	65.67	76.23	65.27	71.04
LLaVA in VLF-Net	90.40	77.76	81.10	80.56	82.46
w/o ConvNeXt-to-LLaVA	96.41	84.40	90.68	88.09	89.90
VLF-FFD (Ours)	**97.29**	**85.41**	**92.04**	**89.15**	**90.97**

Table 5: Ablation study results for the external detector. Notably, CNN-based models outperform the Transformer-based ViT, and VLF-FFD improves the performance of all external detectors.

Method	Test Set AUC (%)				Avg.
	CDF2	DFDC	DFDCP	FFIW	
EfficientNet-B4 [24]	93.18	72.42	86.15	84.83	84.15
+ VLF-FFD	95.38	81.46	88.21	87.50	88.14
ViT-B/16 [74]	93.64	79.66	85.73	83.92	85.74
+ VLF-FFD	95.13	82.82	87.44	86.17	87.89
ConvNeXt-B [17]	96.08	84.26	90.20	87.67	89.55
+ VLF-FFD	**97.29**	**85.41**	**92.04**	**89.15**	**90.97**

Table 6: Ablation study results for VLFM. The proposed architecture consistently surpasses all alternative variants, highlighting its superior ability to integrate visual and textual information.

Method	Test Set AUC (%)				Avg.
	CDF2	DFDC	DFDCP	FFIW	
w/o Cross-Attentions	96.54	84.60	91.25	88.45	90.21
w/o $\mathrm{CA}_{\mathrm{img}\rightarrow\mathrm{text}}$	96.91	85.28	91.62	88.93	90.69
w/o $\mathrm{CA}_{\mathrm{text}\rightarrow\mathrm{img}}$	96.86	85.08	91.49	88.39	90.46
w/ Addition	96.94	84.91	91.73	88.54	90.53
w/ Concatenation	97.07	85.00	91.81	88.84	90.68
VLFM (Ours)	**97.29**	**85.41**	**92.04**	**89.15**	**90.97**

The three-stage training pipeline is configured as follows: In Stage 1, the external detector is trained for 200 epochs using the AdamW optimizer [73], a batch size of 64, and an initial learning rate of 5×10^{-5}, with linear learning rate decay commencing at epoch 100 to encourage stable convergence. Stage 2 involves training the MLLM for 6 epochs with a batch size of 32. In Stage 3, we train the VLFM for 5 epochs with a batch size of 128, again employing the AdamW optimizer and a learning rate of 5×10^{-5}. All experiments are implemented using the PyTorch framework and executed on a cluster of eight RTX 3090 GPUs. Additional implementation details are provided in Appendix B.1.

4.2 Results

Cross-Dataset Evaluation. Table 1 compares our approach with recent SOTA face forgery detectors across multiple unseen datasets. The proposed VLF-FFD outperforms both traditional and MLLM-based methods, demonstrating its exceptional generalization capability. This superior performance can be attributed to the effective integration of visual and textual information within our framework.

Intra-Dataset Evaluation. Table 2 presents the intra-dataset performance comparison between VLF-FFD and existing methods, underscoring the superior detection ability of our approach. Figure 5 illustrates the attention maps produced by VLFM alongside their corresponding explanatory outputs. Notably, the attention maps consistently focus on facial regions exhibiting forgery artifacts, which closely align with the areas described in the generated explanations. This strong correspondence demonstrates the effective integration of visual and textual modalities achieved by VLF-FFD.

4.3 Ablation Studies

In this section, we systematically discuss key components of our work: the proposed EFF++ dataset, our approach to integrating the MLLM within the VLF-FFD framework, our choice of external detectors, and the specific architectural designs of the VLFM. Additional ablation studies, such as investigations into LLM selection and the three-stage training strategy, are provided in Appendix B.2.

EFF++. To evaluate the impact of the EFF++ dataset on forgery detection performance, we conduct experiments by training VLF-Net on four distinct datasets during the second stage of our training pipeline. These datasets include: (1) DDVQA [53], a video-level, explainability-focused extension of FF++; (2) a frame-level dataset generated using only the basic prompt (w/o CFAD & MTS); (3) an EFF++ variant created without the CFAD method (w/o CFAD); and (4) an EFF++ variant produced without the MTS method (w/o MTS). As summarized in Table 3, the EFF++ dataset achieves the

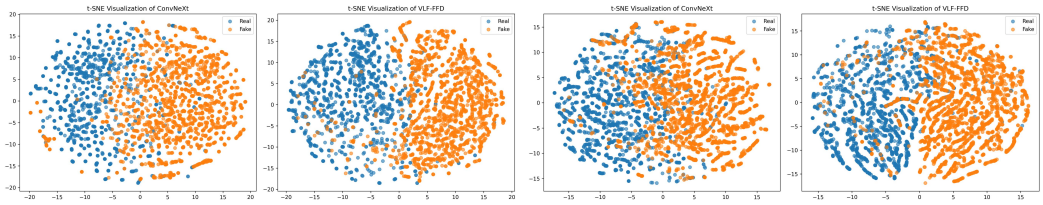

t-SNE results on CDF2 t-SNE results on DFDCP

Figure 6: t-SNE visualizations of feature representations produced by ConvNeXt and VLF-FFD models on the CDF2 and DFDCP datasets. The proposed VLF-FFD yields more distinct and well-separated clusters, highlighting its superior discriminative capability compared to ConvNeXt.

highest overall performance, validating our design choices. Specifically, frame-level annotations help mitigate overfitting, CFAD enables precise identification and localization of forgery artifacts, and MTS enriches explanations with authoritative information that goes beyond common-sense reasoning.

MLLM. We conduct a series of ablation studies to quantify the advantages of embedding the MLLM within our VLF-FFD framework, rather than using it as a standalone forgery detector. Specifically, we compare our method against four variants: (1) the original LLaVA model without any fine-tuning (Pre-trained LLaVA); (2) the LLaVA model fine-tuned on the EFF++ dataset (Fine-tuned LLaVA); (3) the LLaVA model in VLF-Net, where prediction scores are derived from its textual explanations; and (4) VLF-Net without image embeddings E_C fed into the LLM, effectively removing the connection between ConvNeXt and LLaVA. As Table 4 demonstrates, our fully integrated approach consistently outperforms all alternatives under cross-dataset evaluation. The notably poor performance of both pre-trained and fine-tuned LLaVA models underscores the need for specialized datasets and highlights the crucial role of external detectors in achieving robust MLLM-based face forgery detection.

External Detector. We perform a series of experiments to assess the impact of various external detectors on VLF-FFD's performance. Specifically, we compare ConvNeXt [17] with another CNN-based model, EfficientNet [24], as well as the Transformer-based ViT [74]. We also evaluate the overall performance when each of these architectures is integrated into the VLF-FFD framework. As shown in Table 5, the cross-dataset results highlight two key findings: (1) CNN-based backbones consistently outperform the Transformer-based ViT within our framework, and (2) VLF-FFD substantially enhances the forgery detection capabilities of all external detectors tested. Additionally, t-SNE visualizations [75] in Figure 6 demonstrate that VLF-FFD achieves a clearer separation between real and fake samples than standalone external detectors, highlighting its superior discriminative power.

VLFM. To rigorously assess the effectiveness of VLFM, we conduct comprehensive ablation studies across multiple structural variants. Specifically, we analyze: (1) the overall contribution of cross-attention blocks by removing them entirely (w/o Cross-Attentions); (2) the individual roles of each cross-attention direction by ablating either $\mathrm{CA}_{\mathrm{img}\rightarrow\mathrm{text}}$ or $\mathrm{CA}_{\mathrm{text}\rightarrow\mathrm{img}}$; and (3) the relative advantages of the dot-product feature fusion method compared to alternative strategies, such as addition and concatenation. As shown in Table 6, the cross-dataset evaluations validate the design choices of VLFM, consistently demonstrating their substantial benefits to overall model performance.

5 Conclusion

This paper introduces VLF-FFD, a novel Vision-Language Fusion framework tailored for MLLM-enhanced Face Forgery Detection. Our contributions are twofold. First, we develop EFF++, an explainability-focused extension of the FF++ dataset that incorporates CFAD and MTS methods to generate precise and authoritative textual annotations at the frame level. Second, we propose VLF-Net, an innovative network architecture that facilitates bidirectional interaction between visual and textual modalities. To maximize the effectiveness of VLF-Net, we devise a structured three-stage training pipeline. Through extensive cross-dataset and intra-dataset experiments across five widely adopted benchmarks: CDF2, DFDC, DFDCP, FFIW, and FF++, we demonstrate that VLF-FFD consistently surpasses both traditional approaches and MLLM-based methods. Comprehensive ablation studies further validate the significance of each component within our framework. Collectively, these results establish VLF-FFD as an effective and robust solution for MLLM-driven face forgery detection.

References

[1] Lingzhi Li, Jianmin Bao, Hao Yang, Dong Chen, and Fang Wen. Faceshifter: Towards high fidelity and occlusion aware face swapping. *arXiv preprint arXiv:1912.13457*, 2019.

[2] Yuval Nirkin, Yosi Keller, and Tal Hassner. Fsgan: Subject agnostic face swapping and reenactment. In *Proceedings of the IEEE/CVF International Conference on Computer Vision (ICCV)*, pages 7184–7193, 2019.

[3] Mohammad Rami Koujan, Michail Christos Doukas, Anastasios Roussos, and Stefanos Zafeiriou. Head2head: Video-based neural head synthesis. In *2020 15th IEEE International Conference on Automatic Face and Gesture Recognition (FG 2020)*, pages 16–23, 2020.

[4] Gee-Sern Hsu, Chun-Hung Tsai, and Hung-Yi Wu. Dual-generator face reenactment. In *Proceedings of the IEEE/CVF Conference on Computer Vision and Pattern Recognition (CVPR)*, pages 642–650, June 2022.

[5] Kaede Shiohara, Xingchao Yang, and Takafumi Taketomi. Blendface: Re-designing identity encoders for face-swapping. In *Proceedings of the IEEE/CVF International Conference on Computer Vision (ICCV)*, pages 7634–7644, October 2023.

[6] Junnan Li, Dongxu Li, Silvio Savarese, and Steven Hoi. BLIP-2: Bootstrapping language-image pre-training with frozen image encoders and large language models. In *Proceedings of the 40th International Conference on Machine Learning (ICML)*, volume 202, pages 19730–19742, 23–29 Jul 2023.

[7] Haotian Liu, Chunyuan Li, Qingyang Wu, and Yong Jae Lee. Visual instruction tuning. In *Advances in Neural Information Processing Systems (NeurIPS)*, volume 36, pages 34892–34916, 2023.

[8] Haotian Liu, Chunyuan Li, Yuheng Li, and Yong Jae Lee. Improved baselines with visual instruction tuning. In *Proceedings of the IEEE/CVF Conference on Computer Vision and Pattern Recognition (CVPR)*, pages 26296–26306, June 2024.

[9] Shilong Liu, Hao Cheng, Haotian Liu, Hao Zhang, Feng Li, Tianhe Ren, Xueyan Zou, Jianwei Yang, Hang Su, Jun Zhu, et al. Llava-plus: Learning to use tools for creating multimodal agents. In *Proceedings of The 18th European Conference on Computer Vision (ECCV)*, pages 126–142. Springer, 2024.

[10] Yichen Shi, Yuhao Gao, Yingxin Lai, Hongyang Wang, Jun Feng, Lei He, Jun Wan, Changsheng Chen, Zitong Yu, and Xiaochun Cao. Shield: An evaluation benchmark for face spoofing and forgery detection with multimodal large language models. *arXiv preprint arXiv:2402.04178*, 2024.

[11] Shan Jia, Reilin Lyu, Kangran Zhao, Yize Chen, Zhiyuan Yan, Yan Ju, Chuanbo Hu, Xin Li, Baoyuan Wu, and Siwei Lyu. Can chatgpt detect deepfakes? a study of using multimodal large language models for media forensics. In *Proceedings of the IEEE/CVF Conference on Computer Vision and Pattern Recognition (CVPR) Workshops*, pages 4324–4333, June 2024.

[12] Yize Chen, Zhiyuan Yan, Siwei Lyu, and Baoyuan Wu. X2-dfd: A framework for explainable and extendable deepfake detection. *arXiv preprint arXiv:2410.06126*, 2024.

[13] Peipeng Yu, Jianwei Fei, Hui Gao, Xuan Feng, Zhihua Xia, and Chip Hong Chang. Unlocking the capabilities of vision-language models for generalizable and explainable deepfake detection. *arXiv preprint arXiv:2503.14853*, 2025.

[14] Xiao Guo, Xiufeng Song, Yue Zhang, Xiaohong Liu, and Xiaoming Liu. Rethinking vision-language model in face forensics: Multi-modal interpretable forged face detector. *arXiv preprint arXiv:2503.20188*, 2025.

[15] Andreas Rossler, Davide Cozzolino, Luisa Verdoliva, Christian Riess, Justus Thies, and Matthias Niessner. Faceforensics++: Learning to detect manipulated facial images. In *Proceedings of the IEEE/CVF International Conference on Computer Vision (ICCV)*, October 2019.

[16] Gemini Team, Rohan Anil, Sebastian Borgeaud, Jean-Baptiste Alayrac, Jiahui Yu, Radu Soricut, Johan Schalkwyk, Andrew M Dai, Anja Hauth, Katie Millican, et al. Gemini: a family of highly capable multimodal models. *arXiv preprint arXiv:2312.11805*, 2023.

[17] Zhuang Liu, Hanzi Mao, Chao-Yuan Wu, Christoph Feichtenhofer, Trevor Darrell, and Saining Xie. A convnet for the 2020s. In *Proceedings of the IEEE/CVF Conference on Computer Vision and Pattern Recognition (CVPR)*, pages 11976–11986, June 2022.

[18] Yuezun Li, Xin Yang, Pu Sun, Honggang Qi, and Siwei Lyu. Celeb-df: A large-scale challenging dataset for deepfake forensics. In *Proceedings of the IEEE/CVF Conference on Computer Vision and Pattern Recognition (CVPR)*, June 2020.

[19] Gan Pei, Jiangning Zhang, Menghan Hu, Zhenyu Zhang, Chengjie Wang, Yunsheng Wu, Guangtao Zhai, Jian Yang, Chunhua Shen, and Dacheng Tao. Deepfake generation and detection: A benchmark and survey. *arXiv preprint arXiv:2403.17881*, 2024.

[20] Peisong He, Haoliang Li, and Hongxia Wang. Detection of fake images via the ensemble of deep representations from multi color spaces. In *2019 IEEE International Conference on Image Processing (ICIP)*, pages 2299–2303, 2019.

[21] Scott McCloskey and Michael Albright. Detecting gan-generated imagery using saturation cues. In *2019 IEEE International Conference on Image Processing (ICIP)*, pages 4584–4588, 2019.

[22] Hanqing Zhao, Wenbo Zhou, Dongdong Chen, Tianyi Wei, Weiming Zhang, and Nenghai Yu. Multi-attentional deepfake detection. In *Proceedings of the IEEE/CVF Conference on Computer Vision and Pattern Recognition (CVPR)*, pages 2185–2194, June 2021.

[23] Junyi Cao, Chao Ma, Taiping Yao, Shen Chen, Shouhong Ding, and Xiaokang Yang. End-to-end reconstruction-classification learning for face forgery detection. In *Proceedings of the IEEE/CVF Conference on Computer Vision and Pattern Recognition (CVPR)*, pages 4113–4122, 2022.

[24] Kaede Shiohara and Toshihiko Yamasaki. Detecting deepfakes with self-blended images. In *Proceedings of the IEEE/CVF Conference on Computer Vision and Pattern Recognition (CVPR)*, pages 18720–18729, 2022.

[25] Peipeng Yu, Jianwei Fei, Zhihua Xia, Zhili Zhou, and Jian Weng. Improving generalization by commonality learning in face forgery detection. *IEEE Transactions on Information Forensics and Security*, 17:547–558, 2022.

[26] Xinjie Cui, Yuezun Li, Ao Luo, Jiaran Zhou, and Junyu Dong. Forensics adapter: Adapting clip for generalizable face forgery detection. *arXiv preprint arXiv:2411.19715*, 2024.

[27] Alexandros Haliassos, Konstantinos Vougioukas, Stavros Petridis, and Maja Pantic. Lips don't lie: A generalisable and robust approach to face forgery detection. In *Proceedings of the IEEE/CVF Conference on Computer Vision and Pattern Recognition (CVPR)*, pages 5039–5049, June 2021.

[28] Zhihao Gu, Yang Chen, Taiping Yao, Shouhong Ding, Jilin Li, Feiyue Huang, and Lizhuang Ma. Spatiotemporal inconsistency learning for deepfake video detection. In *Proceedings of the 29th ACM International Conference on Multimedia (ACM MM)*, page 3473–3481, 2021.

[29] Zhihao Gu, Yang Chen, Taiping Yao, Shouhong Ding, Jilin Li, and Lizhuang Ma. Delving into the local: Dynamic inconsistency learning for deepfake video detection. In *Proceedings of the AAAI conference on artificial intelligence (AAAI)*, volume 36, pages 744–752, 2022.

[30] Zhihao Gu, Taiping Yao, Yang Chen, Shouhong Ding, and Lizhuang Ma. Hierarchical contrastive inconsistency learning for deepfake video detection. In *Proceedings of the 17th European conference on computer vision (ECCV)*, pages 596–613. Springer, 2022.

[31] Ziming Yang, Jian Liang, Yuting Xu, Xiao-Yu Zhang, and Ran He. Masked relation learning for deepfake detection. *IEEE Transactions on Information Forensics and Security*, 18:1696–1708, 2023.

[32] Chunlei Peng, Zimin Miao, Decheng Liu, Nannan Wang, Ruimin Hu, and Xinbo Gao. Where deepfakes gaze at? spatial–temporal gaze inconsistency analysis for video face forgery detection. *IEEE Transactions on Information Forensics and Security*, 19:4507–4517, 2024.

[33] Daichi Zhang, Zihao Xiao, Shikun Li, Fanzhao Lin, Jianmin Li, and Shiming Ge. Learning natural consistency representation for face forgery video detection. In *Proceedings of the 18th European Conference on Computer Vision (ECCV)*, pages 407–424. Springer, 2024.

[34] Chuangchuang Tan, Yao Zhao, Shikui Wei, Guanghua Gu, Ping Liu, and Yunchao Wei. Frequency-aware deepfake detection: Improving generalizability through frequency space domain learning. In *Proceedings of the AAAI Conference on Artificial Intelligence (AAAI)*, volume 38, pages 5052–5060, 2024.

[35] Yuyang Qian, Guojun Yin, Lu Sheng, Zixuan Chen, and Jing Shao. Thinking in frequency: Face forgery detection by mining frequency-aware clues. In *Proceedings of the 16th European conference on computer vision (ECCV)*, pages 86–103. Springer, 2020.

[36] Hengduo Li, Zuxuan Wu, Abhinav Shrivastava, and Larry S. Davis. 2d or not 2d? adaptive 3d convolution selection for efficient video recognition. In *Proceedings of the IEEE/CVF Conference on Computer Vision and Pattern Recognition (CVPR)*, pages 6155–6164, June 2021.

[37] Gengyun Jia, Meisong Zheng, Chuanrui Hu, Xin Ma, Yuting Xu, Luoqi Liu, Yafeng Deng, and Ran He. Inconsistency-aware wavelet dual-branch network for face forgery detection. *IEEE Transactions on Biometrics, Behavior, and Identity Science*, 3(3):308–319, 2021.

[38] Jiaming Li, Hongtao Xie, Lingyun Yu, and Yongdong Zhang. Wavelet-enhanced weakly supervised local feature learning for face forgery detection. In *Proceedings of the 30th ACM International Conference on Multimedia (ACM MM)*, page 1299–1308, 2022.

[39] Changtao Miao, Zichang Tan, Qi Chu, Huan Liu, Honggang Hu, and Nenghai Yu. F2trans: High-frequency fine-grained transformer for face forgery detection. *IEEE Transactions on Information Forensics and Security*, 18:1039–1051, 2023.

[40] Siran Peng, Tianshuo Zhang, Li Gao, Xiangyu Zhu, Haoyuan Zhang, Kai Pang, and Zhen Lei. Wmamba: Wavelet-based mamba for face forgery detection. *arXiv preprint arXiv:2501.09617*, 2025.

[41] Tianchen Zhao, Xiang Xu, Mingze Xu, Hui Ding, Yuanjun Xiong, and Wei Xia. Learning self-consistency for deepfake detection. In *Proceedings of the IEEE/CVF International Conference on Computer Vision (ICCV)*, pages 15023–15033, 2021.

[42] Juan Hu, Xin Liao, Jinwen Liang, Wenbo Zhou, and Zheng Qin. Finfer: Frame inference-based deepfake detection for high-visual-quality videos. In *Proceedings of the AAAI conference on artificial intelligence (AAAI)*, volume 36, pages 951–959, 2022.

[43] Xiao Guo, Xiaohong Liu, Zhiyuan Ren, Steven Grosz, Iacopo Masi, and Xiaoming Liu. Hierarchical fine-grained image forgery detection and localization. In *Proceedings of the IEEE/CVF Conference on Computer Vision and Pattern Recognition (CVPR)*, pages 3155–3165, June 2023.

[44] Baojin Huang, Zhongyuan Wang, Jifan Yang, Jiaxin Ai, Qin Zou, Qian Wang, and Dengpan Ye. Implicit identity driven deepfake face swapping detection. In *Proceedings of the IEEE/CVF Conference on Computer Vision and Pattern Recognition (CVPR)*, pages 4490–4499, June 2023.

[45] Zhiyuan Yan, Yong Zhang, Yanbo Fan, and Baoyuan Wu. Ucf: Uncovering common features for generalizable deepfake detection. In *Proceedings of the IEEE/CVF International Conference on Computer Vision (ICCV)*, pages 22412–22423, October 2023.

[46] Yuanhao Zhai, Tianyu Luan, David Doermann, and Junsong Yuan. Towards generic image manipulation detection with weakly-supervised self-consistency learning. In *Proceedings of the IEEE/CVF International Conference on Computer Vision (ICCV)*, pages 22390–22400, 2023.

[47] Zhiyuan Yan, Yuhao Luo, Siwei Lyu, Qingshan Liu, and Baoyuan Wu. Transcending forgery specificity with latent space augmentation for generalizable deepfake detection. In *Proceedings of the IEEE/CVF Conference on Computer Vision and Pattern Recognition (CVPR)*, pages 8984–8994, June 2024.

[48] Zhengchao Huang, Bin Xia, Zicheng Lin, Zhun Mou, Wenming Yang, and Jiaya Jia. Ffaa: Multimodal large language model based explainable open-world face forgery analysis assistant. *arXiv preprint arXiv:2408.10072*, 2024.

[49] Niki Maria Foteinopoulou, Enjie Ghorbel, and Djamila Aouada. A hitchhiker's guide to fine-grained face forgery detection using common sense reasoning. In *Advances in Neural Information Processing Systems (NeurIPS)*, volume 37, pages 2943–2976, 2024.

[50] Junhao Xu, Jingjing Chen, Yang Jiao, Jiacheng Zhang, Zhiyu Tan, Hao Li, and Yu-Gang Jiang. Identity-aware vision-language model for explainable face forgery detection. *arXiv preprint arXiv:2504.09439*, 2025.

[51] Alec Radford, Jong Wook Kim, Chris Hallacy, Aditya Ramesh, Gabriel Goh, Sandhini Agarwal, Girish Sastry, Amanda Askell, Pamela Mishkin, Jack Clark, Gretchen Krueger, and Ilya Sutskever. Learning transferable visual models from natural language supervision. In *Proceedings of the 38th International Conference on Machine Learning (ICML)*, volume 139, pages 8748–8763, 18–24 Jul 2021.

[52] Anichur Rahman, Shahariar Hossain Mahir, Md Tanjum An Tashrif, Airin Afroj Aishi, Md Ahsan Karim, Dipanjali Kundu, Tanoy Debnath, Md Abul Ala Moududi, and MD Eidmum. Comparative analysis based on deepseek, chatgpt, and google gemini: Features, techniques, performance, future prospects. *arXiv preprint arXiv:2503.04783*, 2025.

[53] Yue Zhang, Ben Colman, Xiao Guo, Ali Shahriyari, and Gaurav Bharaj. Common sense reasoning for deepfake detection. In *Proceedings of the 18th European Conference on Computer Vision (ECCV)*, pages 399–415. Springer, 2024.

[54] Justus Thies, Michael Zollhofer, Marc Stamminger, Christian Theobalt, and Matthias Niessner. Face2face: Real-time face capture and reenactment of rgb videos. In *Proceedings of the IEEE Conference on Computer Vision and Pattern Recognition (CVPR)*, June 2016.

[55] Justus Thies, Michael Zollhöfer, and Matthias Nießner. Deferred neural rendering: Image synthesis using neural textures. *ACM Transactions on Graphics*, 38(4):1–12, 2019.

[56] Albert Q. Jiang, Alexandre Sablayrolles, Arthur Mensch, Chris Bamford, Devendra Singh Chaplot, Diego de las Casas, Florian Bressand, Gianna Lengyel, Guillaume Lample, Lucile Saulnier, Lélio Renard Lavaud, Marie-Anne Lachaux, Pierre Stock, Teven Le Scao, Thibaut Lavril, Thomas Wang, Timothée Lacroix, and William El Sayed. Mistral 7b. *arXiv preprint arXiv:2310.06825*, 2023.

[57] Edward J. Hu, Yelong Shen, Phillip Wallis, Zeyuan Allen-Zhu, Yuanzhi Li, Shengli Wang, Weiyang Chen, and William Wang. Lora: Low-rank adaptation of large language models. In *International Conference on Learning Representations (ICLR)*, 2022.

[58] Ke Sun, Hong Liu, Qixiang Ye, Yue Gao, Jianzhuang Liu, Ling Shao, and Rongrong Ji. Domain general face forgery detection by learning to weight. In *Proceedings of the AAAI conference on artificial intelligence (AAAI)*, volume 35, pages 2638–2646, 2021.

[59] Ke Sun, Taiping Yao, Shen Chen, Shouhong Ding, Jilin Li, and Rongrong Ji. Dual contrastive learning for general face forgery detection. In *Proceedings of the AAAI Conference on Artificial Intelligence (AAAI)*, volume 36, pages 2316–2324, 2022.

[60] Weiming Bai, Yufan Liu, Zhipeng Zhang, Bing Li, and Weiming Hu. Aunet: Learning relations between action units for face forgery detection. In *Proceedings of the IEEE/CVF Conference on Computer Vision and Pattern Recognition (CVPR)*, pages 24709–24719, 2023.

[61] Nicolas Larue, Ngoc-Son Vu, Vitomir Struc, Peter Peer, and Vassilis Christophides. Seeable: Soft discrepancies and bounded contrastive learning for exposing deepfakes. In *Proceedings of the IEEE/CVF International Conference on Computer Vision (ICCV)*, pages 21011–21021, October 2023.

[62] Dat Nguyen, Nesryne Mejri, Inder Pal Singh, Polina Kuleshova, Marcella Astrid, Anis Kacem, Enjie Ghorbel, and Djamila Aouada. Laa-net: Localized artifact attention network for quality-agnostic and generalizable deepfake detection. In *Proceedings of the IEEE/CVF Conference on Computer Vision and Pattern Recognition (CVPR)*, pages 17395–17405, June 2024.

[63] Jiahe Tian, Cai Yu, Xi Wang, Peng Chen, Zihao Xiao, Jiao Dai, Jizhong Han, and Yesheng Chai. Real appearance modeling for more general deepfake detection. In *Proceedings of the 18th European Conference on Computer Vision (ECCV)*, pages 402–419, 2024.

[64] Jiaran Zhou, Yuezun Li, Baoyuan Wu, Bin Li, Junyu Dong, et al. Freqblender: Enhancing deepfake detection by blending frequency knowledge. In *Advances in Neural Information Processing Systems (NeurIPS)*, volume 37, pages 44965–44988, 2024.

[65] Xinghe Fu, Zhiyuan Yan, Taiping Yao, Shen Chen, and Xi Li. Exploring unbiased deepfake detection via token-level shuffling and mixing. In *Proceedings of the AAAI Conference on Artificial Intelligence (AAAI)*, 2025.

[66] Elahe Soltandoost, Richard Plesh, Stephanie Schuckers, Peter Peer, and Vitomir Štruc. Extracting local information from global representations for interpretable deepfake detection. In *Proceedings of the Winter Conference on Applications of Computer Vision (WACV) Workshops*, pages 1629–1639, February 2025.

[67] Brian Dolhansky, Joanna Bitton, Ben Pflaum, Jikuo Lu, Russ Howes, Menglin Wang, and Cristian Canton Ferrer. The deepfake detection challenge (dfdc) dataset. *arXiv preprint arXiv:2006.07397*, 2020.

[68] Brian Dolhansky, Russ Howes, Ben Pflaum, Nicole Baram, and Cristian Canton Ferrer. The deepfake detection challenge (dfdc) preview dataset. *arXiv preprint arXiv:1910.08854*, 2019.

[69] Tianfei Zhou, Wenguan Wang, Zhiyuan Liang, and Jianbing Shen. Face forensics in the wild. In *Proceedings of the IEEE/CVF Conference on Computer Vision and Pattern Recognition (CVPR)*, pages 5778–5788, June 2021.

[70] Lingzhi Li, Jianmin Bao, Ting Zhang, Hao Yang, Dong Chen, Fang Wen, and Baining Guo. Face x-ray for more general face forgery detection. In *Proceedings of the IEEE/CVF Conference on Computer Vision and Pattern Recognition (CVPR)*, June 2020.

[71] Jianwei Fei, Yunshu Dai, Peipeng Yu, Tianrun Shen, Zhihua Xia, and Jian Weng. Learning second order local anomaly for general face forgery detection. In *Proceedings of the IEEE/CVF Conference on Computer Vision and Pattern Recognition (CVPR)*, pages 20270–20280, June 2022.

[72] Jia Deng, Wei Dong, Richard Socher, Li-Jia Li, Kai Li, and Li Fei-Fei. Imagenet: A large-scale hierarchical image database. In *2009 IEEE Conference on Computer Vision and Pattern Recognition (CVPR)*, pages 248–255, 2009.

[73] Ilya Loshchilov and Frank Hutter. Decoupled weight decay regularization. *arXiv preprint arXiv:1711.05101*, 2017.

[74] Alexey Dosovitskiy, Lucas Beyer, Alexander Kolesnikov, Dirk Weissenborn, Xiaohua Zhai, Thomas Unterthiner, Mostafa Dehghani, Matthias Minderer, Georg Heigold, Sylvain Gelly, Jakob Uszkoreit, and Neil Houlsby. An image is worth 16x16 words: Transformers for image recognition at scale. *arXiv preprint arXiv:2010.11929*, 2020.

[75] Laurens Van der Maaten and Geoffrey Hinton. Visualizing data using t-sne. *Journal of machine learning research*, 9(11), 2008.

[76] Davis E King. Dlib-ml: A machine learning toolkit. *The Journal of Machine Learning Research*, 10:1755–1758, 2009.

[77] Jiankang Deng, Jia Guo, Evangelos Ververas, Irene Kotsia, and Stefanos Zafeiriou. Retinaface: Single-shot multi-level face localisation in the wild. In *Proceedings of the IEEE/CVF Conference on Computer Vision and Pattern Recognition (CVPR)*, June 2020.

[78] Alexander Buslaev, Vladimir I Iglovikov, Eugene Khvedchenya, Alex Parinov, Mikhail Druzhinin, and Alexandr A Kalinin. Albumentations: fast and flexible image augmentations. *Information*, 11(2):125, 2020.

[79] Wei-Lin Chiang, Zhuohan Li, Zi Lin, Ying Sheng, Zhanghao Wu, Hao Zhang, Lianmin Zheng, Siyuan Zhuang, Yonghao Zhuang, Joseph E. Gonzalez, Ion Stoica, and Eric P. Xing. Vicuna: An open-source chatbot impressing gpt-4 with 90%* chatgpt quality, March 2023.

[80] Aaron Grattafiori, Abhimanyu Dubey, Abhinav Jauhri, Abhinav Pandey, Abhishek Kadian, Ahmad Al-Dahle, Aiesha Letman, Akhil Mathur, Alan Schelten, Alex Vaughan, et al. The llama 3 herd of models. *arXiv preprint arXiv:2407.21783*, 2024.

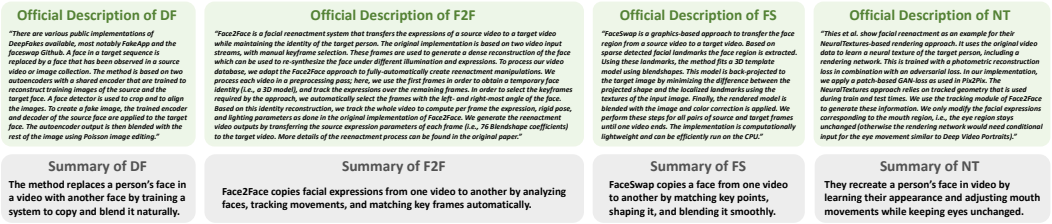

Figure 7: Official descriptions of the manipulation techniques and their MTS-generated summaries.

A Supplementary Information on EFF++

A.1 CFAD

For each identity, we extract frames and crop faces from both the real video and its four fake versions, using identical settings to ensure consistency for the CFAD method. Because the real and fake videos may differ in length, we first determine the minimum frame count among the five videos. We then evenly sample frames from the start-up to this minimum frame index in each video, establishing a clear correspondence between real and fake sequences. For face cropping, we apply the strategy outlined in Appendix B.1, ensuring uniformity between each real video frame and its fake counterparts.

A.2 MTS

Figure 7 presents the official descriptions of the four manipulation techniques used in the FF++ dataset, together with their corresponding summaries produced by MTS. Notably, the generated summaries are clear, concise, and non-technical, making them accessible to a wide audience.

A.3 Final Annotation Generation

Figure 8 presents several annotation examples from the EFF++ dataset. The textual annotations accurately describe the forgery artifacts present in fake images and provide authoritative explanations of the manipulation techniques used. For real video frames, we use the following prompt to produce textual annotations: *"As a face forgery detection expert, you will receive a real image. Please provide a concise explanation of why it is real in no more than 40 words. Begin with 'This/The image/face'."*

B Supplementary Information on Experiments

B.1 Implementation Details

SBI. The SBI framework [24] synthesizes fake face images from real samples by emulating the deepfake generation process. First, a real image is processed by two components: the Source-Target Generator (STG) and the Mask Generator (MG). The STG applies a series of image transformations to create pseudo source and target images, while the MG produces a blending mask based on pre-detected facial landmarks, which is then augmented to enhance diversity. Finally, the pseudo source and target images are blended using the generated mask, resulting in a pseudo-fake face sample.

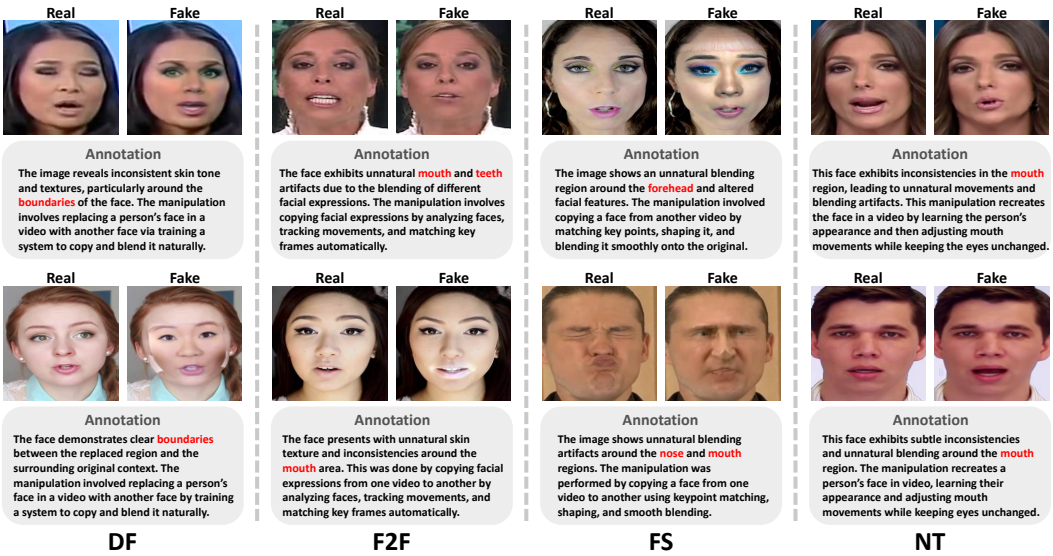

Figure 8: Example annotations of fake samples from the EFF++ dataset. Each textual annotation precisely identifies the forgery artifacts and explains the specific manipulation technique applied.

Table 7: Ablation study results for the LLM, validating the correctness of our design choice.

Method	Test Set AUC (%)				Avg.
	CDF2	DFDC	DFDCP	FFIW	
Vicuna-7B [79]	96.70	84.95	91.38	88.23	90.32
Llama-3-8B [80]	97.22	**85.46**	91.90	88.69	90.82
Mistral-7B [56]	**97.29**	85.41	**92.04**	**89.15**	**90.97**

Table 8: Ablation study results for training strategy, demonstrating the superiority of our method.

Method	Test Set AUC (%)				Avg.
	CDF2	DFDC	DFDCP	FFIW	
One-Stage	84.08	72.50	81.62	71.49	77.42
Two-Stage	95.91	83.87	90.47	87.58	89.46
Three-Stage	**97.29**	**85.41**	**92.04**	**89.15**	**90.97**

Preprocessing. The 81-point facial landmark predictor from Dlib [76] is used to extract facial landmarks, which are required only during the training phase. For face detection, RetinaFace [77] is employed to generate facial bounding boxes. During training, the bounding box is cropped with a random margin between 4% and 20%, whereas a fixed margin of 12.5% is applied during inference. Additionally, for face cropping in CFAD, we employ a random margin between 4% and 20%.

Data Augmentation. The image processing toolbox introduced in [78] is utilized for data augmentation. Within the STG, transformations such as RGBShift, HueSaturationValue, RandomBrightnessContrast, Downscale, and Sharpen are applied to generate pseudo source and target images. Furthermore, for real samples during training under the SBI framework, as well as for all samples in other training scenarios, augmentations such as ImageCompression, RGBShift, HueSaturationValue, and RandomBrightnessContrast are employed. These augmentations expose the model to a wider range of image variations, thereby improving its ability to generalize to previously unseen data.

Settings for Training Stage 2. In the second training stage, we freeze the external detector and fine-tune the MLLM. Specifically, we set the rank and alpha parameters for LoRA tuning [57] to 128 and 256, respectively. The initial learning rate for both the projectors and LoRA layers is set to 1×10^{-5} and is decayed to zero via a cosine schedule starting from the first iteration. The entire MLLM is trained using bfloat16 precision, with gradient accumulation performed after each iteration.

Other Details. During training under the SBI framework, we sample eight frames from each real video. For other training scenarios, we sample 32 frames from each real video and eight frames from each fake video to maintain a balanced ratio of positive and negative samples. During testing, we sample 32 frames per video. If a frame contains multiple detected faces, we apply the classification model to each face individually and use the highest fakeness score as the predicted confidence for that frame. Within VLF-Net, the visual feature map from the penultimate stage of the ConvNeXt network

Table 9: Ablation study results on the number of cross-modal fusion layers in VLFM.

Fusion Layers (L)	Test Set AUC (%)				Avg.
	CDF2	DFDC	DFDCP	FFIW	
1	97.13	85.24	91.53	89.01	90.73
2	**97.29**	**85.41**	**92.04**	89.15	**90.97**
3	97.03	85.36	91.52	**89.46**	90.84
4	97.01	84.80	91.42	88.96	90.55

is sent to the MLLM, while the feature map from the final stage is passed to the VLFM. Additionally, we utilize multi-head cross-attention blocks in the VLFM, with the number of heads set to 16.

B.2 Ablation Studies

LLM. We compare our selected LLM, Mistral-7B [56], with two popular models: Vicuna-7B [79] and Llama-3-8B [80]. The cross-dataset evaluations, shown in Table 7, validate our design choice.

Training Strategy. We evaluate our three-stage training pipeline against two alternative strategies: (1) one-stage training, in which the external detector, MLLM, and VLFM are trained simultaneously, and (2) two-stage training, where the external detector is first optimized using the SBI framework, followed by joint training of the remaining VLF-Net components. As summarized in Table 8, our three-stage training strategy achieves significantly better performance than the other two approaches, clearly demonstrating its superior effectiveness in maximizing the potential of VLF-Net.

VLFM. We evaluate the impact of varying the number of cross-modal fusion layers in VLFM. The cross-dataset results in Table 9 indicate that using two fusion layers yields optimal performance.

C Discussions

C.1 Strengths

This paper exhibits two main advantages. First, the EFF++ dataset provides frame-level textual annotations that not only precisely describe forgery artifacts but also offer authoritative explanations of the manipulation techniques used. Second, the VLF-Net enables rich bidirectional interaction between visual and textual modalities, leading to SOTA performance in face forgery detection.

C.2 Limitation

This work focuses on frame-level face forgery detection. Therefore, the proposed framework may not be readily applicable to video-level face forgery detection without further adaptation.